

Accepted Manuscript

Chemometrical-electrochemical investigation for comparing inhibitory effects of quercetin and its sulfonamide derivative on human carbonic anhydrase II: Theoretical and experimental evidence

Reza Khodarahmi, Shaya Khateri, Hadi Adibi, Vahid Nasirian, Mehdi Hedayati, Elahe Faramarzi, Shokoufeh Soleimani, Hector C. Goicoechea, Ali R. Jalalvand



PII: S0141-8130(19)33531-7

DOI: <https://doi.org/10.1016/j.ijbiomac.2019.06.093>

Reference: BIOMAC 12599

To appear in: *International Journal of Biological Macromolecules*

Received date: 13 May 2019

Revised date: 12 June 2019

Accepted date: 13 June 2019

Please cite this article as: R. Khodarahmi, S. Khateri, H. Adibi, et al., Chemometrical-electrochemical investigation for comparing inhibitory effects of quercetin and its sulfonamide derivative on human carbonic anhydrase II: Theoretical and experimental evidence, *International Journal of Biological Macromolecules*, <https://doi.org/10.1016/j.ijbiomac.2019.06.093>

This is a PDF file of an unedited manuscript that has been accepted for publication. As a service to our customers we are providing this early version of the manuscript. The manuscript will undergo copyediting, typesetting, and review of the resulting proof before it is published in its final form. Please note that during the production process errors may be discovered which could affect the content, and all legal disclaimers that apply to the journal pertain.

Chemometrical-electrochemical investigation for comparing inhibitory effects of quercetin and its sulfonamide derivative on human carbonic anhydrase II: Theoretical and experimental evidence

Reza Khodarahmi^a, Shaya Khateri^a, Hadi Adibi^b, Vahid Nasirian^c, Mehdi Hedayati^d, Elahe Faramarzi^e, Shokoufeh Soleimani^e, Hector C. Goicoechea^f, Ali R. Jalalvand^{e,*}

^a*Medical Biology Research Center, Health Technology Institute, Kermanshah University of Medical Sciences, Kermanshah, Iran*

^b*Pharmaceutical Sciences Research Center, Kermanshah University of Medical Sciences, Kermanshah, Iran*

^c*Department of Chemistry and Physics, Louisiana State University in Shreveport, Shreveport, LA, USA*

^d*Cellular and Molecular Endocrine Research Center, Research Institute for Endocrine Sciences, Shahid Beheshti University of Medical Sciences, Tehran, Iran*

^e*Research Center of Oils and Fats, Kermanshah University of Medical Sciences, Kermanshah, Iran*

^f*Laboratorio de Desarrollo Analítico y Quimiometría (LADAQ), Catedra de Química Analítica I, Universidad Nacional del Litoral, Ciudad Universitaria, CC242 (S3000ZAA), Santa Fe, Argentina*

**Corresponding Author: E-mail Addresses:*

ali.jalalvand1984@gmail.com; alireza.jalalvand@kums.ac.ir (A.-R. Jalalvand)

Abstract

This paper reports results of a valuable study on investigation of inhibitory effects of the sulfonamide derivative of quercetin (QD) on human carbonic anhydrase II (CA-II) by electrochemical and chemometrical approaches. To achieve this goal, a glassy carbon electrode (GCE) was chosen as the sensing platform and different electrochemical techniques such as cyclic voltammetry (CV), differential pulse voltammetry (DPV), linear sweep voltammetry (LSV) and electrochemical impedance spectroscopy (EIS) were used to investigate and comparing inhibitory effects of quercetin (Q) and QD on CA-II. By the use of EQUISPEC, SPECFIT, SQUAD and REACTLAB as efficient hard-modeling algorithms, bindings of Q and QD with CA-II were investigated and the results confirmed that the QD inhibited the CA-II stronger than Q suggesting a highly relevant role of QD's-SO₂NH₂ group in inhibiting activity and also was confirmed by docking studies. Finally, a novel EIS technique based on interaction of Q and CA-II was developed for sensitive electroanalytical determination of CA-II and in this section of our study, the sensitivity of the developed electroanalytical methodology was improved by the modification of the GCE was with multi-walled carbon nanotubes-ionic liquid.

Keywords: Quercetin; Quercetin derivative; Human carbonic anhydrase II.

1. Introduction

Carbonic anhydrases are zinc containing enzymes which are able to catalyze the reversible hydration of carbon dioxide to bicarbonate and hydrogen ions [1-4]. Human carbonic anhydrase II (CA-II, Fig. 1A) is a single chain enzyme having 259 amino acid residues with a molecular mass of 29 kDa [5]. The CA-II has a high catalytic activity with a very high affinity to sulfonamide derivatives and its active site contains a zinc ion which is located in a cone-shaped cavity surrounded by three histidyl residues and a solvent molecule [6]. Aromatic sulfonamides can inhibit the CA-II [7], therefore, in the present study, we are going to investigate the inhibitory effects of the sulfonamide derivative of quercetin (Q) on CA-II. Molecular structures of the Q and its sulfonamide derivative (QD) are shown in Fig. 1B and C.

Fig. 1

There is a variety of instrumental techniques such as UV-Vis spectrophotometry [8], FT-IR [9], electrochemistry [10], capillary electrophoresis [11], high performance liquid chromatography (HPLC) [12] and nuclear magnetic resonance (NMR) [13] which can be used to investigate the binding of a small molecule with a biological macromolecule such as an enzyme. Among the mentioned techniques, electrochemical methods are simple, inexpensive, fast, sensitive, selective, repeatable and reproducible which make them to be suitable for investigation of small molecule-enzyme interactions. Sometimes, electrochemical methods are assisted by chemometrical approaches which can help them to be improved [14-18]. When an investigation focused on small molecule-enzyme interactions is assisted by chemometric methods, valuable information could be extracted which cannot be obtained by the use of conventional methods.

In the present study, we are going to investigate the inhibitory effects of the QD on human carbonic anhydrase II by recording different types of electrochemical data such as differential pulse voltammetry (DPV), cyclic voltammetry (CV), linear sweep voltammetry (LSV) and electrochemical impedance spectroscopy (EIS) and analysing them by chemometric hard-modeling algorithms including EQUISPEC, SPECFIT, SQUAD and REACTLAB and conventional methods. The results can help us to clarify the role of QD's $-SO_2NH_2$ group for

inhibiting the activity of CA-II which can be further investigated by molecular docking methods. Finally, by the modification of a glassy carbon electrode (GCE) as the sensing platform by multiwalled carbon nanotubes-1-ethyl-3-methylimidazolium bis(trifluoromethylsulfonyl) imide (MWCNTs-IL) to increase its sensitivity, an indirect electroanalytical method based on Q-CA-II interactions will be developed for sensitive determination of CA-II. The schematic representation of the steps of the present study can be seen in Scheme 1.

Scheme 1

2. Experimental

2.1. Chemicals and solutions

The Q, CA-II, Tris-HCl, MWCNTs, IL, alumina, dimethylformamide (DMF), potassium ferrocyanide, potassium ferricyanide and the other chemicals used in this study were purchased from Sigma-Aldrich and QD was synthesized by our research group. A Tris-HCl buffer solution (TBS) with a concentration of 0.1 M and pH 7.4 containing 0.05 M sodium chloride to keep its ionic strength constant was prepared in doubly distilled water (DDW) and kept in a refrigerator. Stock solutions of Q, QD and CA-II were prepared in TBS (0.1 M, pH 7.4) and working solutions of Q, QD and CA-II were prepared by appropriate dilution of their stock solutions. Suitable amounts of solid powders of potassium ferrocyanide and potassium ferricyanide were used to prepare a 5.0 mM $[\text{Fe}(\text{CN})_6]^{3-/4-}$ in 0.5 mM KCl. To prepare the MWCNTs-IL, 20 mg MWCNTs was mixed with 1 mL DMF containing 20 μL IL and ultrasonicated for 1 hour. To prepare CA-II-MWCNTs-IL, 0.5 mL 2×10^{-4} M CA-II was added to 0.5 mL MWCNTs-IL.

2.2. Instrument and software

All types of electrochemical data were recorded by an Autolab PGSTAT302N-high performance under controlling by the NOVA software (version 2.1). A GCE, a Pt wire and an Ag/AgCl electrode were purchased from Metrohm which were used as working, counter and reference electrode, respectively. The scanning electron microscopic (SEM) images was taken by using a MIRA3TESCAN-XMU. pH adjustments were performed by an ELMEIRON pH meter (CP-411). Calculations based on EQUISPEC were run in MATLAB environment (version 7.5). SPECFIT, SQUAD and REACTLAB were available in the achieve of our laboratory or downloaded from the internet. The chemical structures of the Q and QD were constructed by

Hyperchem package 8.0. The crystal structure of CA-II was downloaded from Brookhaven Protein Data Bank. The molecular docking Arguslab 4.0.1 program [19] was employed to docking studies. LIGPLOT [208], was used for analyzing the enzyme-ligand interactions.

2.3. Fabrication of the biosensor

Prior to the modification of the GCE, it was well-polished on alumina slurry by a silky pad and rinsed with DDW. Then, the electrode was immersed into a beaker containing ethanol and ultrasonicated for 30 min and finally, rinsed with DDW. To fabricate the biosensor for biosensing of CA-II, the cleaned GCE was used as the platform of the biosensor and 15 μ L MWCNTs-IL was drop-casted onto its surface and left to be dried under a warm air provided by a hair-dryer. Finally, the biosensor was rinsed with DDW and covered until analysis time.

2.4. Electrochemical titrations

For all types of electrochemical techniques including DPV, CV, LSV and EIS two different titrations including Q with CA-II and QD with CA-II were performed. 5 mL of CA-II with a known concentration was added to the electrochemical cell and different volumes of Q or QD were added to the cell. After gentle stirring each solution for 1 min, its electrochemical response was recorded.

3. Results and discussion

3.1. Morphological characterization of the platform for biosensing of CA-II

The SEM is a very useful technique for characterization of the modifications applied to a bare GCE to fabricate a biosensor. Therefore, we have used it for morphological characterization of MWCNTs-IL/GCE which was used as the biosensing platform for CA-II and the results are shown in Fig. 2. By comparing Fig. 2A and B, it can be clearly observed that the GCE surface has been covered by a pretty layer of MWCNTs-IL in which the tubes have been twined around each other and well-distributed.

Fig. 2

All the experiments related to the investigation of interaction of Q and QD with CA-II were performed at the surface of the bare GCE and at the final step of our study to increase the sensitivity of the

GCE for biosensing of CA-II, it was modified by MWCNTs-IL. Therefore, in next section, electrochemical behavior of Q and QD at the GCE will be investigated.

3.2. Electrochemical behavior of Q and QD at the GCE

The CV as a very useful technique was used to investigate electrochemical behavior of Q and QD at the surface of the GCE. The CV responses of Q and QD at different scan rates (v) are shown in Fig. S1. As can be seen, the CV currents of Q and QD were linearly increased with increasing the rate of scanning potentials which are shown in Fig. S1B and D. These observations confirmed that the redox reactions for Q and QD at the surface of the GCE were surface-controlled processes.

3.3. Investigation of interactions of Q and QD with CA-II

3.3.1. CV studies

Useful information about interactions of small molecules with enzymes can be obtained by CV as one of the most important electroanalytical techniques. Therefore, CV was used to investigate interactions of Q and QD with CA-II at the surface of the GCE. Fig. 3A and B shows the CV responses of 1×10^{-4} M Q and QD upon addition of CA-II in the range of $0-1 \times 10^{-4}$ M, respectively. As can be seen, the current intensities are decreasing with increasing CA-II concentration which may be related to the interaction of Q and QD with CA-II. Some phenomena such as increasing the viscosity of the solution by the addition of CA-II or blockage of the GCE surface by CA-II adsorption can decrease the peak intensities. Therefore, more investigations are needed to clarify the reason of the decrease in peak currents. According to the previous work published in the literature [21], we have performed an interesting investigation based on using $[\text{Fe}(\text{CN})_6]^{3-/4-}$ in the absence and presence of CA-II to clarify our observations. To achieve this goal, CVs of 5.0 mM $[\text{Fe}(\text{CN})_6]^{3-/4-}$ which cannot interact with CA-II were recorded at the surface of the GCE in the absence of CA-II (Fig. 3C, curve *a*) and presence of CA-II (Fig. 3C, curve *b*). As can be seen, the CV response of $[\text{Fe}(\text{CN})_6]^{3-/4-}$ in the presence of CA-II didn't change significantly which confirmed that the decrease in peak currents of Q in the presence of increasing concentration of CA-II was related to the binding of Q and QD to CA-II. Interaction of Q or QD with CA-II

causes formation of a bulky complex which slowly diffuses. Our observations were further clarified by the EIS technique and the results are shown in Fig. 3D. The EISs of 5.0 mM $[\text{Fe}(\text{CN})_6]^{3-/4-}$ at the surface of the GCE in the absence of CA-II (Fig. 3D, curve *a*) and in the presence of CA-II (Fig. 3D, curve *b*) were recorded. As can be seen, the EIS response of $[\text{Fe}(\text{CN})_6]^{3-/4-}$ in the presence of CA-II didn't change significantly which was in a good agreement with the CV results. This step was carried out to show that the decrease in peak currents was related to the complex formation and not due to blockage of the electrode surface by an adsorbed layer of the enzyme.

Fig. 3

3.3.1.1. Determination of the binding constants of Q and QD to CA-II

Here, the binding constants of Q and QD to CA-II were determined by CV and to achieve this goal, 15 μL CA-II-MWCNTs-IL was drop-casted onto the surface of the cleaned GCE and left to be dried. Then, this electrode was immersed into 5 mL TBS (0.1 M, pH 7.4) and Q or QD was added to it in the range of 5×10^{-4} M and the CVs were recorded (not shown). It was observed that the peak intensity was increased by increasing Q or QD concentration (C_Q or C_{QD}) and then, reached to saturation values. Binding constants related to the binding of Q to CA-II ($K_{b,Q}$) and QD to CA-II ($K_{b,QD}$) were computed according to the following equation [22]:

$$C/I = (1/K_b I_{\max}) + (C/I_{\max}) \quad (1)$$

where C , I , I_{\max} , and K_b are concentration of Q or QD, peak current, maximum peak current and the binding constant at CA-II-MWCNTs-IL/GCE surface, respectively. Regression of C/I on C at CA-II-MWCNTs-IL/GCE obeyed the following equations: $C_Q/I = 72.61 + 15.88C_Q$ and $C_{QD}/I = 48.11 + 13.01C_{QD}$ for Q and QD, respectively. The $K_{b,Q}$ and $K_{b,QD}$ values were calculated from the intercept of these equation which were to be 1.14×10^2 and $2.47 \times 10^2 \text{ mol}^{-1} \text{ L}$, respectively.

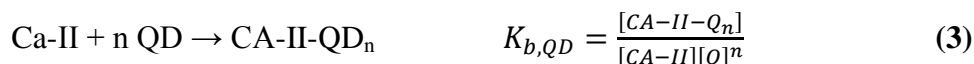
3.3.2. LSV studies

The LSV is another important electrochemical technique which has been used to investigate interactions of Q and QD with CA-II. The LSVs related to the addition of CA-II to Q and QD are shown in Fig. S2A and B, respectively. As can be seen, the LSVs of Q and QD are decreased by the addition of CA-II which may be

related to their interactions with the enzyme. Some phenomena such as adsorption of the enzyme onto the electrode surface can also decrease the peak intensities which must be clarified. It has been proven that when interactions of a small molecule with a biological macromolecule such as an enzyme with quite a low concentration and a short accumulation time is occurred, only a low area from the electrode surface about 10% maybe covered [23]. Therefore, the decrease in peak currents are related to the interaction and complex formation of Q and QD with CA-II. Embedding Q or QD within the CA-II structure decreases the equilibrium concentration of Q or QD in solution. Therefore, the LSV results confirmed that interactions of Q and QD with CA-II led to complex formation.

3.3.3. DPV studies

In order to further investigation of interactions of Q and QD with CA-II, the DPV data related to the titration of Q and QD with CA-II were recorded and the results are shown in Fig. S3. As can be seen, the DPV data show that with increasing concentration of CA-II, the peak intensities are decreasing which confirm the CV and LSV results. If it is assumed that the complexes CA-II-Q_m and CA-II-QD_n are formed by binding Q and QD to CA-II, respectively, the following reactions can be written:



The following equations can help us to obtain stoichiometry of the complexes and binding constants [24,25]:

$$\log \left[\frac{\Delta I}{(\Delta I_{\max} - \Delta I)} \right] = m \log K_{b,Q} + m \log [\text{Q}] \quad (4)$$

$$\log \left[\frac{\Delta I}{(\Delta I_{\max} - \Delta I)} \right] = n \log K_{b,QD} + n \log [\text{QD}] \quad (5)$$

where ΔI represents the difference in the oxidative current in the absence or presence of CA-II, and the maximum value of ΔI is ΔI_{\max} . By linear regression of $\log \left[\frac{\Delta I}{(\Delta I_{\max} - \Delta I)} \right]$ on $\log [\text{Q}]$ or $\log [\text{QD}]$, we will be able to calculate stoichiometry of the complexes and binding constant values. By doing the mentioned actions, m

and n were calculated to be ~ 1 and $K_{b,Q}$ and $K_{b,QD}$ were obtained as 1.21×10^2 and $2.34 \times 10^2 \text{ mol}^{-1} \text{ L}$, respectively.

3.3.4. EIS studies

The EIS is a very interesting electrochemical technique which can be used for characterization, determination, complexation and the other purposes. Here, we are going to use it for investigation of interactions of Q and QD with CA-II. To achieve these goals, the EIS spectra of the GCE immersed into the redox probe having a constant concentration of Q or QD were recorded upon increasing concentration of CA-II and the results are shown in Fig. 4. As can be seen, the charge transfer resistance (R_{ct}) of the EIS curves were increased by the addition of CA-II to Q or QD which may be related to the adsorption of the complex formed upon insertion of Q or QD within the CA-II structure at the electrode surface which hindered the accessibility of the $[\text{Fe}(\text{CN})_6]^{3-}$ to the electrode surface [26-28]. Therefore, the change in the EIS response of the GCE upon interaction of Q or QD with CA-II confirmed complex formation by the interaction of Q or QD with CA-II. The EIS is a very sensitive electroanalytical technique which can also be used for quantitative purposes [29], and in next sections, we will develop a novel EIS method based the results of this section for sensitive biosensing of CA-II.

Fig. 4

3.3.5. Determination of the stoichiometry of the complexes by mole-ratio method

Mole-ratio plots are very useful plots which can help us to obtain valuable information about stoichiometry of the complex species formed under interactions of Q or QD with CA-II. By plotting the currents of LSVs and DPVs obtained from titration of Q or QD with CA-II versus mole-ratio ($[\text{CA-II}]/[\text{Q}]$ or $[\text{CA-II}]/[\text{QD}]$), mole-ratio plots were obtained which are shown in Fig. 5. As can be seen, the plots are inflected at $[\text{CA-II}]/[\text{Q}] \sim 0.5$ and $[\text{CA-II}]/[\text{QD}] \sim 0.5$ which confirm formation of CA-II-Q₂ and CA-II-QD₂. The results of this section will help us to define models for hard-modeling algorithms in chemometric studies which will be explained in more details in next sections.

Fig. 5

3.3.6. Chemometric studies

3.3.6.1. Determination of the number of species by principal component analysis (PCA)

The PCA is a well-known chemometric approach which can help us to obtain number of species involved in a system [30]. Therefore, by performing the PCA on the LSV and DPV data, the number of species involved in the interaction of Q and QD with CA-II were determined and the results are shown in Fig. S4. As can be seen, for all the datasets, three main species were detected which were related to the free Q or QD, CA-II and one complex species. The results obtained in this section were compatible with those obtained from mole-ratio method. These results will be used to define models for hard-modeling of the electrochemical data in next section.

3.3.6.2. Hard-modeling of the electrochemical data

Here, we have used some chemometric hard-modeling algorithms such as EQUISPEC, SPECFIT, SQUAD and REACTLAB to investigate interactions of Q and QD with CA-II which helped us to verify the results obtained from previous sections about nature of the species and binding constant values ($K_{b,Q}$ and $K_{b,QD}$). The models were defined according to the formation of one complex species (CA-II-Q₂ or CA-II-QD₂) and estimation of $K_{b,Q}$ and $K_{b,QD}$ was performed according to the results obtained by the direct analysis of the electrochemical data. The results obtained by the modeling of the electrochemical data with the help of EQUISPEC, SPECFIT, SQUAD and REACTLAB have been collected in Table 1. All the models were defined according to CA-II-Q₂ or CA-II-QD₂ as complex species and then, the binding constants were estimated and finally, for each data fitting procedure, the best model with the minimum sum of squares was chosen. As can be seen, hard-modeling of the electrochemical data showed that the complex formed by binding of QD with CA-II was stronger than the complex formed by the binding of Q with CA-II which was related to the highly relevant role of QD's -SO₂NH₂ group which must be further verified in next sections.

Table 1

3.3.7. Molecular docking studies

Here, the Arguslab program was used to obtain more information about interactions of Q and QD with CA-II. After docking Q and QD with CA-II, the residues of CA-II which interacted with Q and QD were detected and the results are shown in Fig. 6. The residues of CA-II which interacted with Q were including Asn 253, Arg

254, Pro 195, Tyr 194, Thr 193, Gln 255, Lys 257 and Asp 41 which as can be seen in Fig. 6A. As can be seen in Fig. 6B, the residues of CA-II which interacted with QD were including Glu 187, Leu 189, Leu 185, Arg 182, Tyr 51, Val 49, Ser 48, Leu 47 and Pro 46. Interactions of Q and QD with CA-II were further investigated by LigPlus and the results are shown in Fig. 6C and D, respectively. As can be seen, four amino acid residues of CA-II including Pro 195, Lys 257, Arg 254 and Asn 253 had hydrophobic interactions with Q while six amino acid residues of CA-II including Ser 48, Leu 47, Leu 189, Arg 182, Leu 185 and Pro 186 were hydrophobically interacted with QD. One hydrogen binding was occurred between CA-II and Q and two hydrogen binding were occurred between QD and CA-II. The only difference between Q and QD is the presence of QD's-SO₂NH₂ group in QD structure and as can be seen, more hydrophobic interactions and hydrogen binding were observed in interaction of QD with CA-II. According to docking results, the binding constants related to the interactions of Q and QD with CA-II were calculated to be 1.41×10^2 and 2.57×10^2 mol⁻¹ L, respectively. The docking results confirmed that binding of QD with CA-II was stronger than Q with CA-II which was compatible with results obtained from experimental sections.

Fig. 6

3.4. Developing a novel method for determination of CA-II

According to results of interaction studies, we were going to develop a novel electroanalytical methodology for sensitive determination of CA-II based on EIS measurements. The EIS is a sensitive technique but, to obtain more sensitivity, the GCE was modified with MWCNTs-IL and used as the biosensing platform [31-37]. More details about the biosensing procedure will be given in next sections.

3.4.1. Impedimetric measurements

Binding of Q to CA-II can be used to develop a novel electroanalytical method for determination of CA-II. Therefore, to achieve this goal, the EIS responses of the MWCNTs-IL/GCE immersed into 5.0 mM [Fe(CN)₆]³⁻/⁴⁻ containing 10 μM Q upon increasing concentration of CA-II in the range of 10-190 nM were recorded which are shown in Fig. 7A. As can be seen, the R_{ct} of the EIS responses is gradually increased upon addition of CA-II to the electrochemical cell. According to the change in the EIS response of the MWCNTs-IL/GCE upon

changing concentration of CA-II we have developed a novel and indirect EIS method for determination CA-II. Regression of the ΔR_{ct} values on concentration of CA-II helped us to build a calibration curve which is shown as the inset of Fig. 7A. As can be seen the EIS responses are linearly correlated with concentration of CA-II in two linear ranges of 10-50 nM and 50-190 nM. The sensitivity and limit of detection were calculated to be $9.5 \Omega \text{ nM}^{-1}$ and 12 nM (according to $3SD/m$, where SD is the standard deviation of the intercept and m is the slope of the calibration curve), respectively.

Fig. 7

3.4.2. Selectivity, stability, repeatability and reproducibility of the developed biosensor

In order to investigate selectivity of the MWCNTs-IL/GCE towards determination of CA-II, the EIS response of the sensor to 50 nM CA-II in the presence of 100-fold interfering species including HSA, BSA, cysteine, tyrosine, histidine, valine, glucose, glycine, L-tryptophan, L-tyrosine, citric acid, folic acid and ascorbic acid was recorded. The results showed that the biosensor was able to selective determination of CA-II even in the presence of high concentrations of the interfering species. Stability of the developed biosensor was investigated by weekly recording its response to 50 nM CA-II during seven weeks and the results showed that the biosensor was able to retain 95.5% of its original response which confirmed that the biosensor response was stable (Fig. 7B). In order to investigate the repeatability of the MWCNTs-IL/GCE response, it was applied to the determination 50 nM CA-II for six times during a day and the results showed that a relative standard deviation (RSD) of 3.66% was obtained which confirmed that the biosensor response was repeatable. Reproducibility of the biosensor was investigated by fabrication of six biosensors and applying them to the determination of 50 nM CA-II and the results showed that a RSD value of 3.51% which confirmed that the biosensor response was reproducible.

4. Conclusions

In this work, an interesting study was planned to investigate interactions of Q and QD with CA-II. The study was performed in several steps including direct analysis of electrochemical data, chemometric modeling of

electrochemical data, molecular modeling and determination of CA-II. Direct analysis of electrochemical data confirmed formation of one complex species including CA-II-Q₂ and CA-II-QD₂ and also confirmed that the binding of QD with CA-II was stronger than binding of Q with CA-II. The results obtained by direct analysis of electrochemical data were verified by hard-modeling of the electrochemical data and there was a good agreement between the results. Then, molecular docking studies were performed to further verification of the results of the previous sections. The results obtained by molecular modeling confirmed stronger binding of QD with CA-II. Finally, according to the results obtained by investigation of interactions of Q and QD with CA-II, an indirect EIS method was developed for sensitive determination of CA-II. On the whole combination of experimental and theoretical evidence helped us to develop a thorough study for investigation of interactions of Q and QD with CA-II with applicable results for determination of CA-II.

Acknowledgements

Hereby, we acknowledge the financial supports of this project by research council of Kermanshah University of Medical Sciences.

References

- [1] C.T. Supuran, A. Scozzafava, A. Casini, Carbonic anhydrase inhibitors, *Med. Res. Rev.* 23 (2003) 146-189.
- [2] S. Lindskog, Structure and mechanism of carbonic anhydrase, *Pharmacol. Ther.* 74 (1997) 1-20.
- [3] F. Topal, I. Gulcin, A. Dastan, M. Guney, Novel eugenol derivatives: Potent acetylcholinesterase and carbonic anhydrase inhibitors, *Int. J. Biol. Macromol.* 94 (2017) 845-851.
- [4] M. Boztas, Y. Cetinkaya, M. Topal, I. Gulcin, A. Menzek, E. Sahin, M. Tanc, C.T. Supuran, Synthesis and carbonic anhydrase isoenzymes I, II, IX, and XII inhibitory effects of dimethoxy-bromophenol derivatives incorporating cyclopropane moieties. *J. Med. Chem.* 58 (2015) 640-650.
- [5] R.A. Venters, B.T. Farmer II, C.A. Fierke, L.D. Spicer, Characterizing the use of perdeuteration in NMR studies of large proteins: ^{13}C , ^{15}N and ^1H assignments of human carbonic anhydrase II, *J. Mol. Biol.* 264 (1996) 1101-1116.
- [6] S. Huang, Y. Xue, E. Sauer-Eriksson, L. Chirica, S. Lindskog, B.H. Jonsson, Crystal structure of carbonic anhydrase from *Neisseria gonorrhoeae* and its complex with the inhibitor acetazolamide1, *J. Mol. Biol.* 283 (1998) 301-310.
- [7] S. Terada, K. Katagiri, H. Masu, H. Danjo, Y. Sei, M. Kawahata, M. Tominaga, K. Yamaguchi, I. Azumaya, Polymorphism of aromatic sulfonamides with fluorine groups, *Cryst. Growth Des.* 12 (2012) 2908-2916.
- [8] Y.Y. Yue, X.G. Chen, J. Qin, X.J. Yao, Characterization of the mangiferin–human serum albumin complex by spectroscopic and molecular modeling approaches, *J. Pharm. Biomed. Anal.* 49 (2009) 753-759.
- [9] J.S. Mandeville, E. Froehlich, H.A. Tajmir-Riahi, Study of curcumin and genistein interactions with human serum albumin, *J. Pharm. Biomed. Anal.* 49 (2009) 468-474.
- [10] H.X. Luo, Y. Du, Z.X. Guo, Electrochemistry of N-n-undecyl-N'-(sodium-p-aminobenzenesulfonate) thiourea and its interaction with bovine serum albumin, *Bioelectrochemistry* 74 (2009) 232-235.
- [11] Q.H. Lu, C.D. Ba, D.Y. Chen, Investigating noncovalent interactions of rutin – serum albumin by capillary electrophoresis – frontal analysis, *J. Pharm. Biomed. Anal.* 47 (2008) 888-891.
- [12] C. Bertucci, V. Andrisano, R. Gotti, V. Cavrini, Use of an immobilised human serum albumin HPLC column as a probe of drug–protein interactions: the reversible binding of valproate, *J. Chromatogr. B* 768 (2002) 147-155.
- [13] B. Bojko, A. Sulkowska, M. Maciazek-Jurczyk, J. Rownicka, W.W. Sulkowski, Investigations of acetaminophen binding to bovine serum albumin in the presence of fatty acid: Fluorescence and ^1H NMR studies, *J. Mol. Struct.* 924-926 (2009) 332-337.

- [14] G. Mohammadi, E. Faramarzi, M. Mahmoudi, S. Ghobadi, A.R. Ghiasvand, H.C. Goicoechea, A.R. Jalalvand, Chemometrics-assisted investigation of interactions of Tasmar with human serum albumin at a glassy carbon disk: application to electrochemical biosensing of electro-inactive serum albumin, *J. Pharm. Biomed. Anal.* 156 (2018) 23–35.
- [15] M.B. Gholivand, A.R. Jalalvand, H.C. Goicoechea, M. Omid, Investigation of interaction of nuclear fast red with human serum albumin by experimental and computational approaches, *Spectrochim. Acta A* 115 (2013) 516–527.
- [16] A.R. Jalalvand, S. Ghobadi, H.C. Goicoechea, H.W. Gu, E. Sanchooli, Investigation of interactions of Comtan with human serum albumin by mathematically modeled voltammetric data: A study from bio-interaction to biosensing, *Bioelectrochemistry* 123 (2018) 162-172.
- [17] M.B. Gholivand, A.R. Jalalvand, H.C. Goicoechea, Multivariate analysis for resolving interactions of carbidopa with dsDNA at a fullerene-C₆₀/GCE, *Int. J. Biol. Macromol.* 69 (2014) 369-381.
- [18] M.B. Gholivand, A.R. Jalalvand, H.C. Goicoechea, R. Gargallo, T. Skov, Chemometrics: An important tool for monitoring interactions of vitamin B7 with bovine serum albumin with the aim of developing an efficient biosensing system for the analysis of protein, *Talanta* 132 (2015) 354-365.
- [19] [http:// www.arguslab.com](http://www.arguslab.com).
- [20] A.C. Wallace, R.A. Laskowski, J.M. Thornton, LIGPLOT: A program to generate schematic diagrams of protein-ligand interactions, *Protein Eng.* 8 (1995) 127-134.
- [21] S.F. Wang, T.Z. Peng, C.F. Yang, *Electroanalysis* 14 (2002) 1648-1653.
- [22] X. Ju, Y.K. Ye, Y.L. Zhu, Interaction between Nile blue and immobilized single- or double-stranded DNA and its application in electrochemical recognition, *Electrochim. Acta* 50 (2005) 1361-1367.
- [23] S.S. Kalanur, U. Katrahalli, J. Seetharamappa, Electrochemical studies and spectroscopic investigations on the interaction of an anticancer drug with DNA and their analytical applications, *J. Electroanal. Chem.* 636 (2009) 93-100.
- [24] Y.X. Wang, Y.N. Ni, S. Kokot, Voltammetric behavior of complexation of salbutamol with calf thymus DNA and its analytical application, *Anal. Biochem.* 419 (2011) 76–80.
- [25] S.S. Kalanur, U. Katrahalli, J. Seetharamappa, Electrochemical studies and spectroscopic investigations on the interaction of an anticancer drug with DNA and their analytical applications, *J. Electroanal. Chem.* 636 (2009) 93–100.
- [26] L.P. Lu, L.H. Xu, T.F. Kang, S.Y. Cheng, Investigation of DNA damage treated with perfluorooctane sulfonate (PFOS) on ZrO₂/DDAB active nano-order film, *Biosens. Bioelectron.* 35 (2012) 180-185.
- [27] X. Lin, Y. Ni, S. Kokot, An electrochemical DNA-sensor developed with the use of methylene blue as a redox indicator for the detection of DNA damage induced by endocrine-disrupting compounds, *Anal. Chim. Acta* 867 (2015) 29-37.
- [28] H. Dai, G.F. Xu, L.S. Gong, C.P. Yang, Y.Y. Lin, Y.J. Tong, J.H. Chen, G.N. Chen, Electrochemical detection of triclosan at a glassy carbon electrode modified with carbon nanodots and chitosan, *Electrochim. Acta* 80 (2012) 362–367.
- [29] M.B. Gholivand, A.R. Jalalvand, G. Paimard, H.C. Goicoechea, T. Skov, R. Farhadi, S. Ghobadi, N. Moradi, V. Nasirian, Fabrication of a novel naltrexone biosensor based on a computationally engineered nanobiocomposite, *Int. J. Biol. Macromol.* 70 (2014) 596-605.
- [30] S. Perez, M.J. Culzoni, G.G. Siano, M.D. Gil Garcia, H.C. Goicoechea, M.M. Galera, *Anal. Chem.* 81 (2009) 8335-8346.
- [31] A.R. Jalalvand, A. Haseli, F. Farzadfar, H.C. Goicoechea, Fabrication of a novel biosensor for biosensing of bisphenol A and detection of its damage to DNA, *Talanta* 201 (2019) 350-357.
- [32] M.B. Gholivand, A.R. Jalalvand, H.C. Goicoechea, G. Paimard, T. Skov, Surface exploration of a room-temperature ionic liquid-chitin composite film decorated with electrochemically deposited PdFeNi trimetallic alloy nanoparticles by pattern recognition: an elegant approach to developing a novel biotin biosensor, *Talanta* 131 (2015) 249–258.

- [33] M.B. Gholivand, A.R. Jalalvand, H.C. Goicoechea, Developing a novel computationally designed impedimetric pregabalin biosensor, *Electrochim. Acta* 133 (2014) 123–131.
- [34] M.B. Gholivand, A.R. Jalalvand, H.C. Goicoechea, Computer-assisted electrochemical fabrication of a highly selective and sensitive amperometric nitrite sensor based on surface decoration of electrochemically reduced graphene oxide nanosheets with CoNi bimetallic alloy nanoparticles, *Mater. Sci. Eng. C* 40 (2014) 109–120.
- [35] M.B. Gholivand, A.R. Jalalvand, H.C. Goicoechea, T. Skov, Fabrication of an ultrasensitive impedimetric buprenorphine hydrochloride biosensor from computational and experimental angles, *Talanta* 124 (2014) 27–35.
- [36] A.R. Jalalvand, Fabrication of a novel and high-performance amperometric sensor for highly sensitive determination of ochratoxin A in juice samples, *Talanta* 188 (2018) 225–231.
- [37] A.R. Jalalvand, H.C. Goicoechea, H.W. Gu, An interesting strategy devoted to fabrication of a novel and high performance amperometric sodium dithionite sensor, *Microchem. J.* 144 (2019) 6–12.

Caption to figures:

Fig. 1. Molecular structure of (A) CA-II, (B) Q and (C) QD.

Fig. 2. SEM images of (A) GCE and (B) MWCNTs-IL/GCE.

Fig. 3. (A) CVs of 1×10^{-4} M Q upon addition of CA-II in the range of $0-1 \times 10^{-4}$ M, (B) CVs of 1×10^{-4} M QD upon addition of CA-II in the range of $0-1 \times 10^{-4}$ M (C) CVs of the GCE immersed in 5.0 mM $[\text{Fe}(\text{CN})_6]^{3-/4-}$: (a) in the absence of CA-II and (b) in the presence of 5.0 mM CA-II. (D) EISs of the GCE immersed in 5.0 mM $[\text{Fe}(\text{CN})_6]^{3-/4-}$: (a) in the absence of CA-II and (b) in the presence of 5.0 mM CA-II.

Fig. 4. (A) The EIS spectra recorded by immersing the GCE into 5.0 mM $[\text{Fe}(\text{CN})_6]^{3-/4-}$ containing 5 μM Q upon addition of CA-II in the range of 0-5 μM and (B) the EIS spectra recorded by immersing the GCE into 5.0 mM $[\text{Fe}(\text{CN})_6]^{3-/4-}$ containing 5 μM Q upon addition of CA-II in the range of 0-5 μM .

Fig. 5. Mole-ratio plots: (A) and (B) obtained from DPV data related to the titration of Q with CA-II and QD with CA-II, respectively, (C) and (D) obtained from LSV data related to the titration of Q with CA-II and QD with CA-II, respectively.

Fig. 6. (A) and (B) the outputs of docking of Q and QD with CA-II. (C) and (D) the outputs of LigPlus related to the interactions of Q and QD with CA-II.

Fig. 7. (A) The EIS responses of MWCNTs-IL/GCE immersed into 5.0 mM $[\text{Fe}(\text{CN})_6]^{3-/4-}$ containing 10 μM Q upon increasing concentration of CA-II in the range of 10-190 nM. Inset shows the calibration curve obtained by the regression of ΔR_{ct} of the EIS responses on concentration of CA-II. (B) Recording the response of MWCNTs-IL/GCE to 50 nM CA-II during seven weeks.

Scheme 1. Schematic representation of the steps of the study presented in this work.

Table 1. Data analysis using different chemometrics algorithms.

Algorithm	Type of electrochemical data	$K_{b,Q}$ ($\times 10^2$ mol ⁻¹ L)	$K_{b,QD}$ ($\times 10^2$ mol ⁻¹ L)
SQUAD	DPV	1.38±0.02	2.44±0.04
	LSV	1.33±0.05	2.41±0.03
	CV	1.35±0.03	2.42±0.05
SPECFIT	DPV	1.33±0.03	2.42±0.05
	LSV	1.36±0.06	2.44±0.02
	CV	1.38±0.02	2.41±0.03
EQUISPEC	DPV	1.38±0.03	2.42±0.02
	LSV	1.35±0.04	2.41±0.03
	CV	1.38±0.04	2.41±0.02
REACTLAB	DPV	1.33±0.05	2.44±0.05
	LSV	1.38±0.03	2.44±0.04
	CV	1.38±0.02	2.41±0.02

Highlights

- ✓ Inhibitory effects of Q and QD with Ca-II were compared.
- ✓ Direct analysis of EIS, CV, LSV and DPV was performed.
- ✓ Hard-modeling of electrochemical data as the second step was performed.
- ✓ Molecular modeling was performed to verify the results of experimental section.
- ✓ A novel electroanalytical method was developed for determination of CA-II.

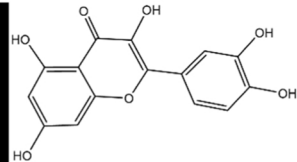
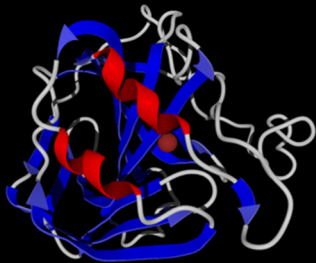
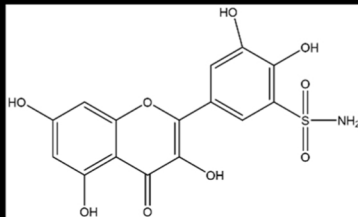
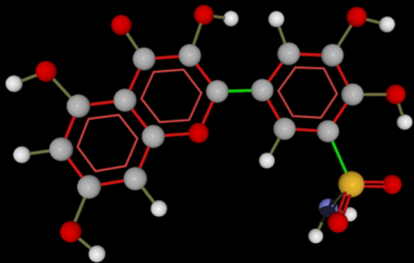
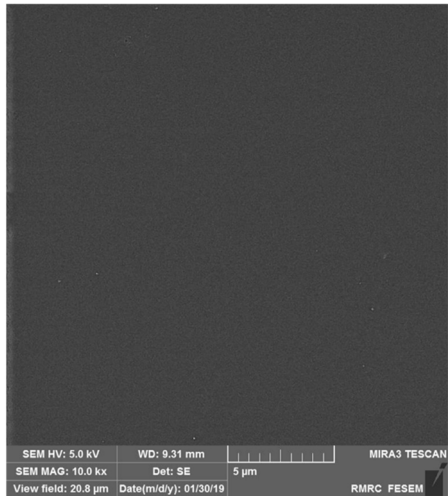
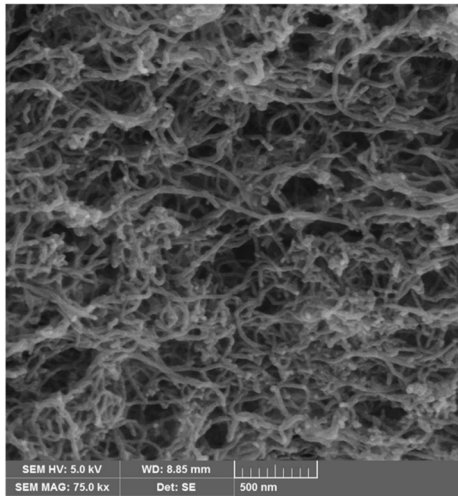
A**B****C**

Figure 1

A**B****Figure 2**

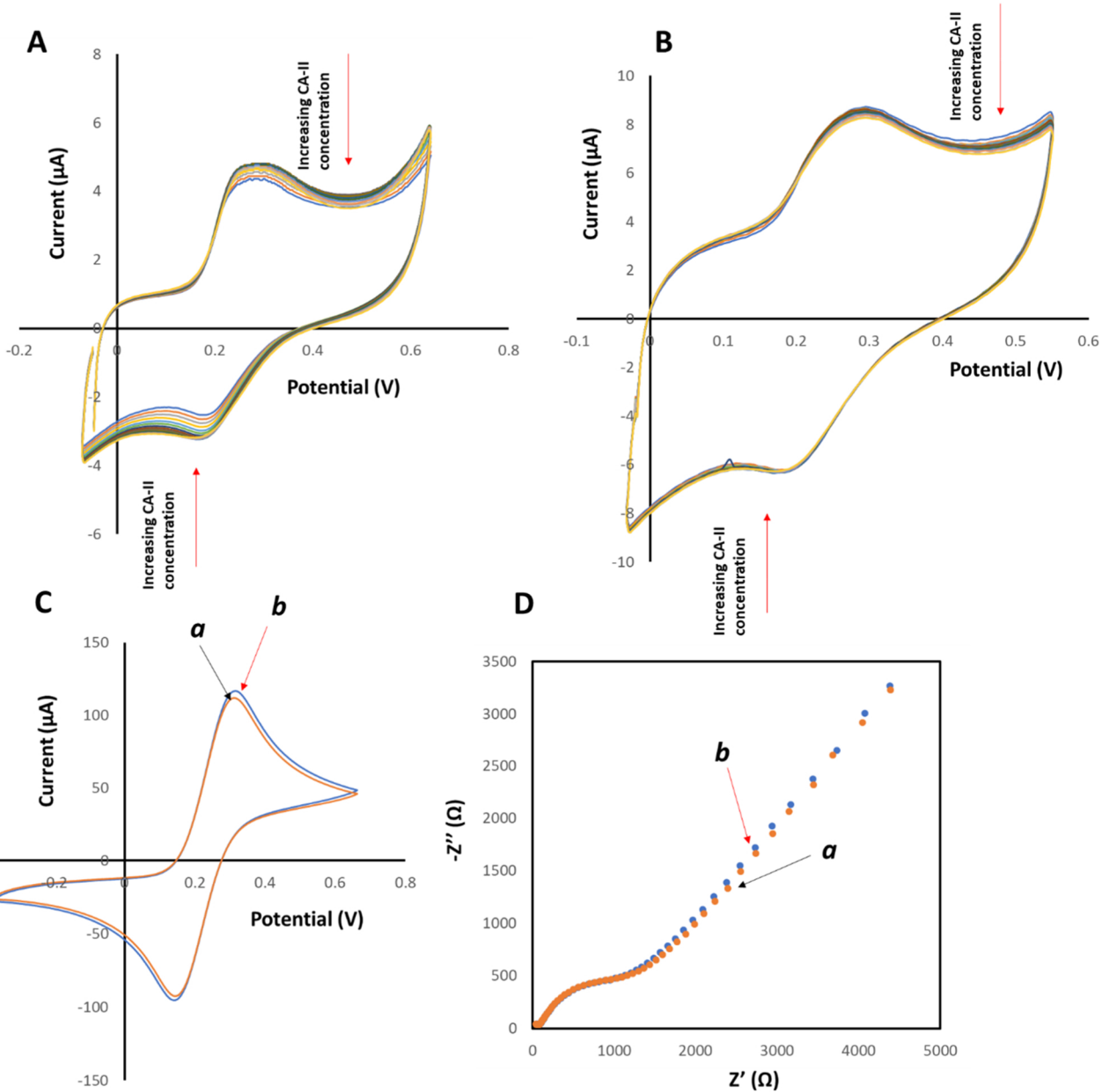


Figure 3

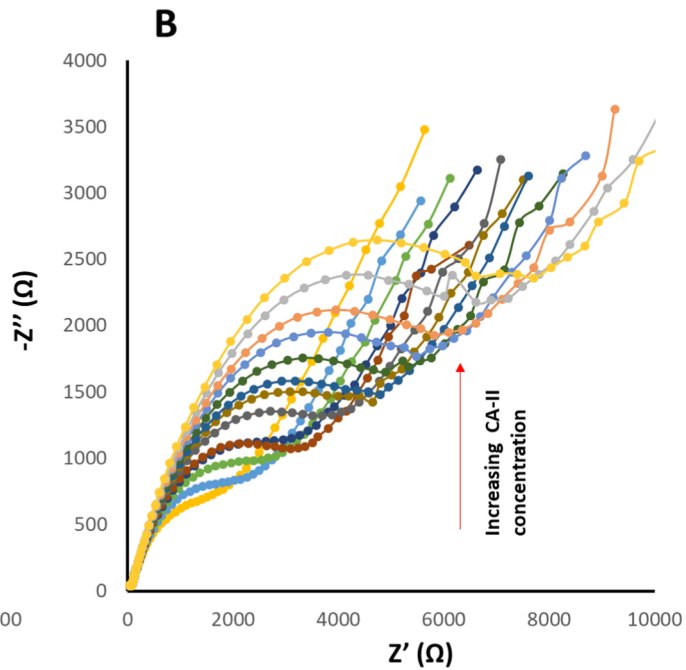
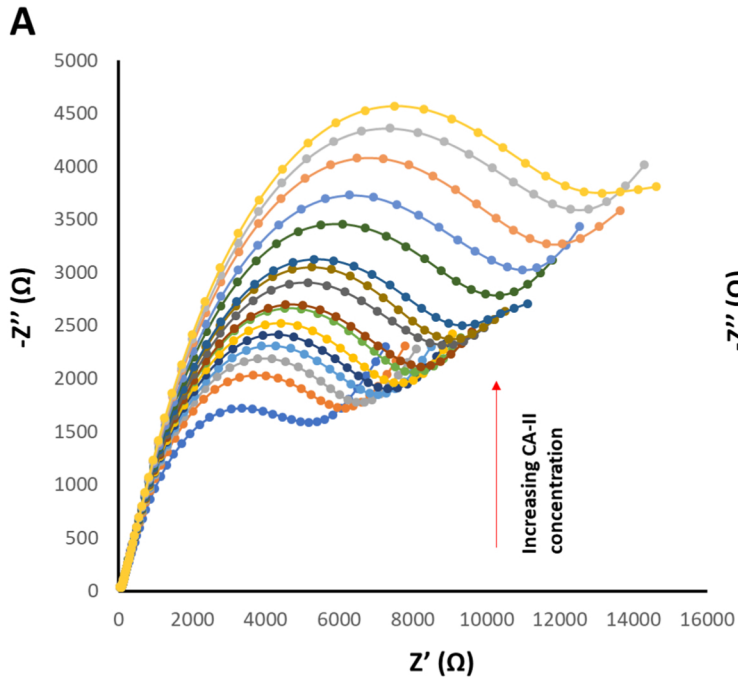


Figure 4

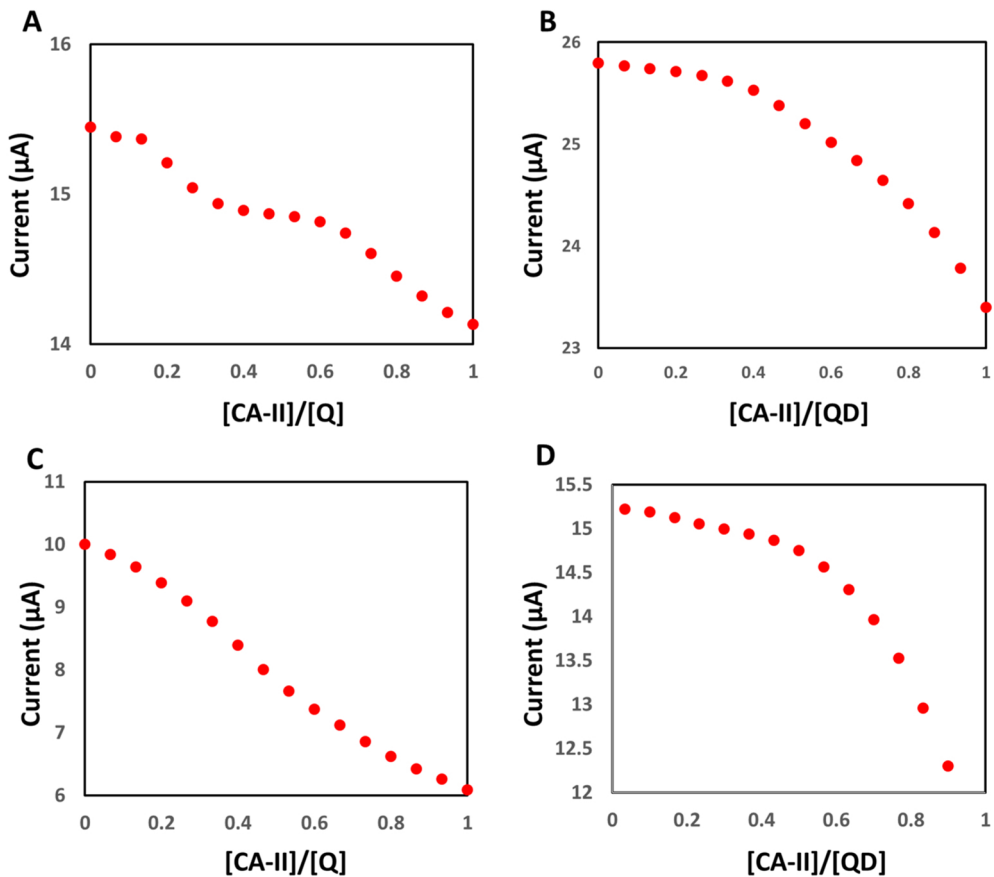
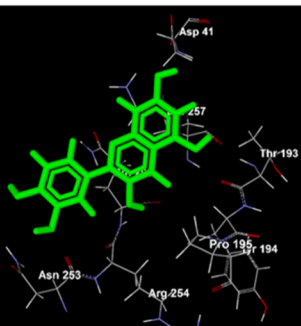
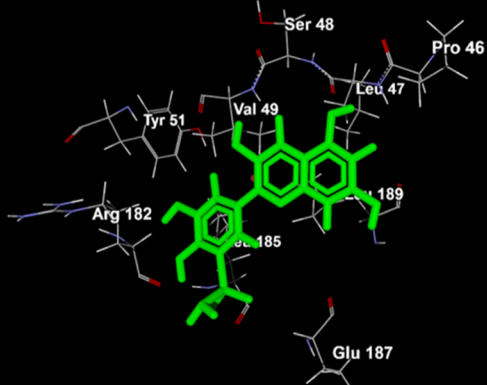


Figure 5

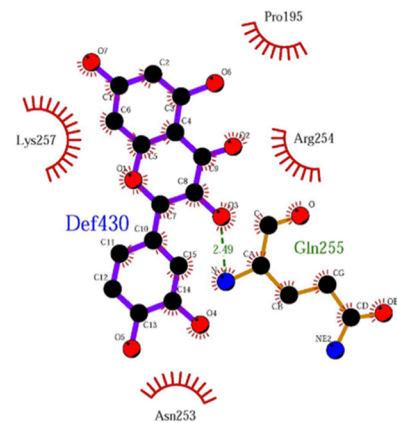
A



B



C



D

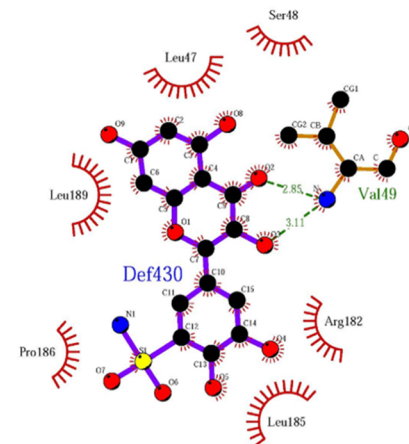


Figure 6

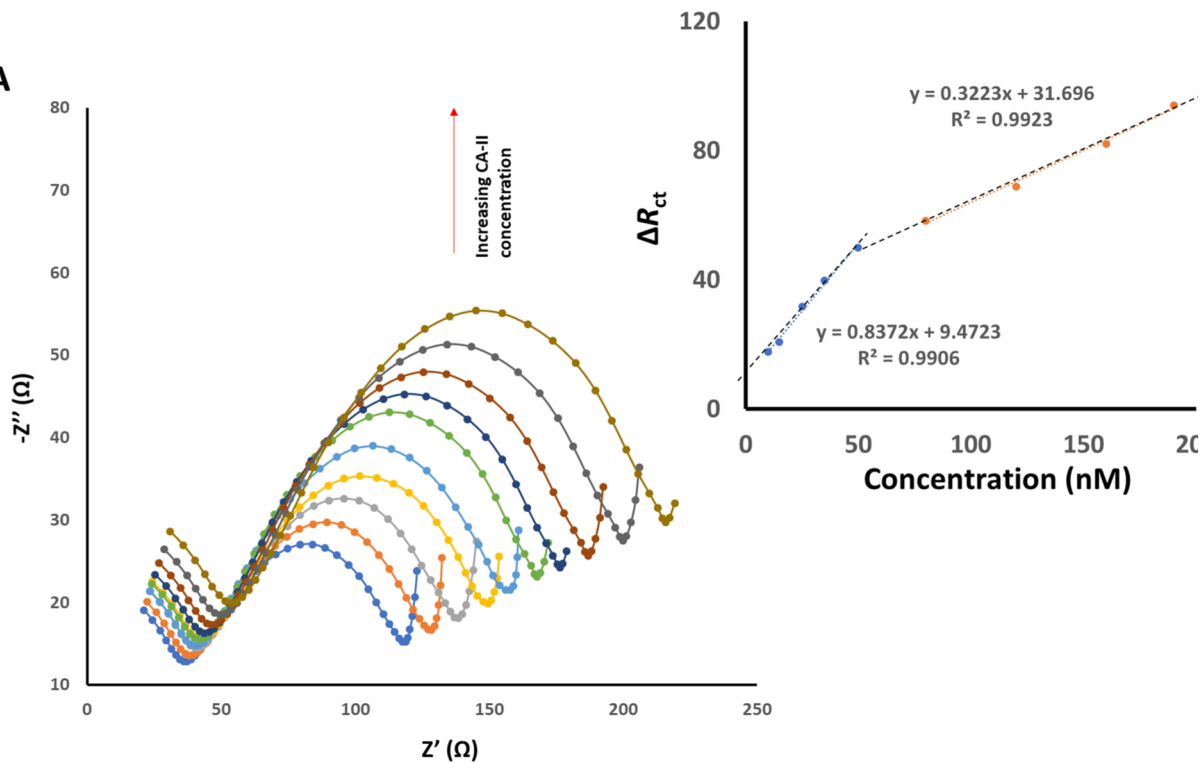
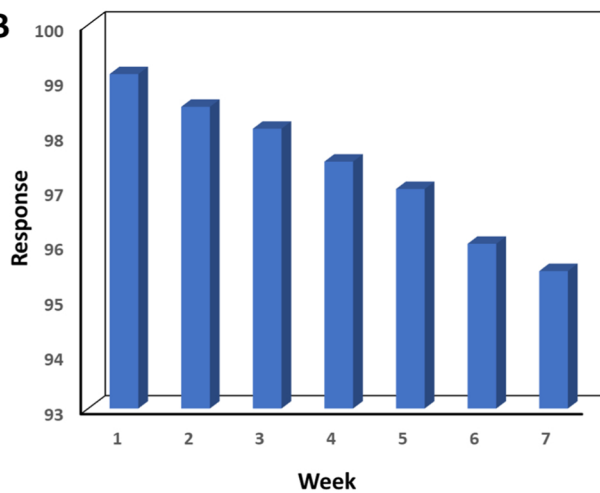
A**B**

Figure 7